

Artificial ferrimagnetic structure and thermal hysteresis in $\text{Gd}_{0.47}\text{Co}_{0.53}/\text{Co}$ multilayers

J. P. Andrés,¹ J. A. González,¹ T. P. A. Hase,² B. K. Tanner,² and J. M. Riveiro¹

¹*Departamento de Física Aplicada, University of Castilla-La Mancha, Ciudad Real 13071, Spain*

²*Department of Physics, University of Durham, South Road, Durham DH1 3LE, United Kingdom*

(Received 15 November 2007; revised manuscript received 25 January 2008; published 3 April 2008)

$\text{Gd}_{0.47}\text{Co}_{0.53}/\text{Co}$ multilayers are presented as an alternative to classical Gd/Fe or Gd/Co to study ferrimagnetic interactions in an artificial multilayered structure with sharper interfaces, since interdiffusion processes are avoided. This system is shown to present all the characteristic features of Gd/Co and Gd/Fe multilayers, as evidenced by the existence of compensation temperatures, spin-flop transitions, and thermal hysteresis. By using this improved structure, we show that the temperatures at which the sample suffers magnetization reversal when cooling or heating during the thermal hysteresis loop depend on the applied field and coercivity, while anisotropy determines the smoothness of the reversal process. Details of the temperature dependency of coercivity and spin-flop fields in this system are also provided.

DOI: [10.1103/PhysRevB.77.144407](https://doi.org/10.1103/PhysRevB.77.144407)

PACS number(s): 75.60.Nt, 75.70.Cn, 75.75.+a, 75.25.+z

I. INTRODUCTION

$\text{Gd}_{1-x}\text{Co}_x$ alloys^{1,2} have been studied extensively in the past due to their ferrimagnetic structure and the possibility of creating thin alloy films with a perpendicular anisotropy that makes them suitable for magnetic recording purposes.³ More recently, artificial Gd/Co and Gd/Fe multilayers have been studied because of the ferrimagnetic structure that exists between the layers below the ordering temperature of the Gd layer. The magnetic superstructure of the multilayers arises from the strong interface interaction between the rare earth and transition metal. Gd is an S ion and shows very small anisotropy, which makes this system ideal for studies of exchange interactions at interfaces. Unfortunately, a strong interdiffusion process occurs when the elements are grown next to each other. This results in a poorly defined interface and therefore a smearing of the properties derived from the interface interactions. This, in turn, complicates the model for their explanation. Surprisingly, there are in the literature many articles about these Gd based systems where this effect is not considered, probably because in spite of the interdiffusion, the main properties of the system are usually preserved.^{4,5} In a previous study of the interdiffusion process between Gd and Co on multilayers, we have shown that this effect converts a nominal Gd/Co sample into a $\text{Gd}_{1-x}\text{Co}_x/\text{Co}$ one.^{6,7} In the alloy, the Gd subnetwork dominates the magnetization of the alloyed layer for $x < 0.8$ (at room temperature), therefore the multilayered system continues to behave as an artificial ferrimagnet even if Gd layers are Co enriched due to interdiffusion. Nevertheless, the thicknesses of the layers and their composition change as a result of the aforementioned interdiffusion leading to rougher and more diffuse interfaces.

In our previous studies,^{8,9} we have quantified the amount of Co that interdiffuses into a $\text{Gd}_{1-x}\text{Co}_x$ layer as a function of the composition of the alloy in the multilayered system $\text{Gd}_{1-x}\text{Co}_x/\text{Co}$ in the range $0 < x < 0.6$. We have shown that although interdiffusion is reduced significantly by employing an alloy with a composition $x=0.37$, it is not negligible until alloy values between $x=0.53$ and $x=0.60$ are used. Although x-ray reflectivity shows a good improvement in the series

with $x=0.37$, polarized neutron reflectivity is still able to detect an interfacial region with separate magnetic properties to the rest of the layer.⁷ This has been also supported by theoretical calculations of the free energy of intermixing.¹⁰ In this paper, we present an alternative to the classic Gd/Co system where interdiffusion is significantly reduced, $\text{Gd}_{0.47}\text{Co}_{0.53}/\text{Co}$, and we show that the main magnetic features of this system, such as the presence of compensation temperatures, spin-flop transitions, or thermal hysteresis,^{11,12} are preserved. This system is closer to the ideal structure assumed in the theoretical calculations, and we present it as a first step to check the validity of such models.¹³ We also take advantage of the improved structure to study the role of anisotropy and coercive field in the thermal hysteresis effect.

II. EXPERIMENT

Samples were grown by sequential sputtering from Co and $\text{Gd}_{0.47}\text{Co}_{0.53}$ targets onto Si (100) substrates at room temperature. Composition of the alloy target was achieved by incorporating small Co pieces onto a Gd sputtering disk. The composition of the resulting sputtering target was quantified by energy dispersive x-ray microanalysis in a scanning electron microscope. The nominal sample structure was $[\text{Co}_t/(\text{Gd}_{0.47}\text{Co}_{0.53})_{100 \text{ \AA}}]_{\times 20}/\text{Co}_t$, with the thickness of the Co layer t ranging from 20 to 50 Å. The main effect of parameter t is to vary the relative magnetization of the two layers and thus control the compensation temperature of the sample. Magnetic properties were measured using conventional vibrating sample magnetometry (VSM) above liquid nitrogen and transverse magneto-optic Kerr effect (MOKE) magnetometry at room temperature. Grazing incidence x-ray reflectivity was performed on the XMaS beamline (BM28) at the European Synchrotron Radiation Facility (ESRF) in Grenoble, with the monochromator tuned to 1.71 Å, the Gd L_{III} absorption edge enhancing the contrast between the layers.

III. RESULTS AND DISCUSSION

A. X-ray analysis

In order to check the structural quality of the samples and the absence of interdiffusion or other processes that could

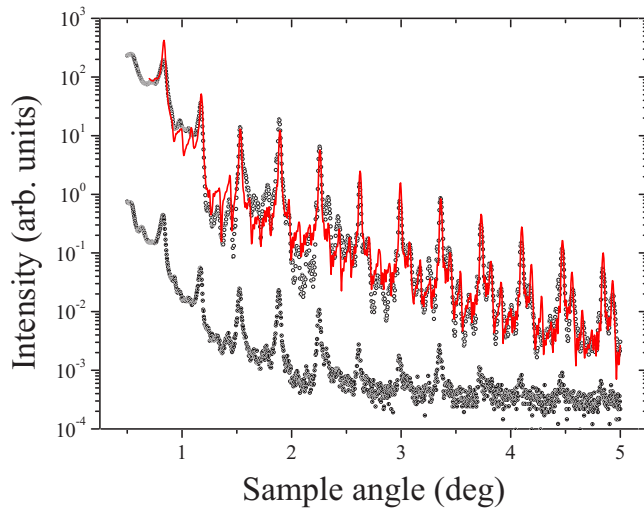


FIG. 1. (Color online) X-ray specular (open symbols) and off-specular (full symbols) reflectivities for the sample with Co thickness $t=35$ Å, together with a fit (red line) to the specular curve.

smear the interfaces, we conducted x-ray reflectivity on representative samples with nominal Co thicknesses $t=35$ and $t=40$ Å. In Fig. 1, we show the specular and off-specular data from the sample with $t=35$ Å together with fits using the fully dynamical model distorted wave Born approximation using the BEDE REFS software.¹⁴ The presence of the Bragg peaks up to 11th order is a clear indication of a good periodicity and low interface roughness, especially when compared with similar results published previously for Gd/Co multilayers.^{5,13,15} Data recorded on resonance show additional fringes in between the Bragg peaks. These arise from a periodic variation in the layer thickness about the nominal values. The Co thickness was 30 ± 5 Å and the alloy layer was 100 ± 5 Å. The data could not be fitted to a simple bilayer model with the peaks in between the Bragg peaks modeled by assuming that the repeat unit was composed of four bilayers. The fitted results indicated that the composition of the alloy in the bulk of the layer was close to nominal Co, $x=(52 \pm 5)\%$. The sensitivity to density variations in a single energy reflectivity fit is low as it tends to be coupled with the interface roughness, determined to be 2.0 ± 0.2 Å for the Co/alloy interface and slightly rougher for the alloy/Co interface, 6.0 ± 0.7 Å. Off-specular data shown in the same figure show that the topological roughness is conformal. On the other hand, the Born analysis on the transverse diffuse data for scans recorded at and away from a Bragg peak (not shown) yields values of the topological roughness to be 1.7 ± 0.5 Å.¹⁶ Thus, we can conclude that there still remains a degree of interdiffusion at the interface, but that is significantly lower than in previous studies.

X-ray specular reflectivity for the sample with a nominal Co thickness of 40 Å is represented in Fig. 2. It did not show any peaks in between the Bragg peaks requiring a simpler model to fit the data. However, the widths of the Bragg peaks were broader indicating a degree of thickness or roughness variation. There was larger variation in the Co thickness (15%) about the nominal value with the alloy layer remaining close to nominal 100 ± 5 Å. The roughnesses were

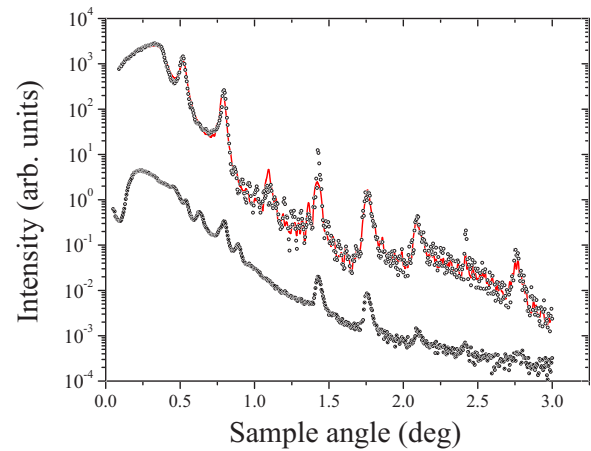


FIG. 2. (Color online) X-ray specular (open symbols) and off-specular (full symbols) reflectivities for the sample with Co thickness $t=40$ Å, together with a fit (red line) to the specular curve.

slightly higher than the $t=35$ Å sample, with both interfaces being 10 ± 5 Å. The composition of the alloy was close to nominal, $x=(53 \pm 2)\%$.

The extra fringes in the low angle region of the off specular arise from harmonic contamination of the beam, only observed when the beam was highly attenuated close to the critical angle. The diffuse scatter was recorded as a function of both in-plane (q_x) and out-of-plane (q_z) scattering vectors in the form of a full reciprocal space map (Fig. 3). Similar data were recorded for all samples studied. The strong streaks of intensity at the Bragg peak positions are what is observed in the off-specular longitudinal scans which probe the diffuse scatter at low small values of q_x . It is clear that the roughness is highly correlated from interface to interface and that these correlations extend over the thickness of the

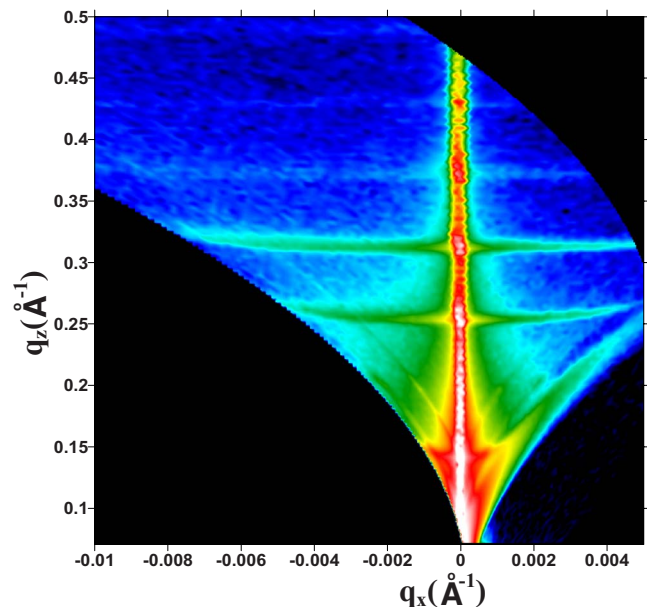


FIG. 3. (Color online) Full reciprocal space map recorded on the sample with $t=40$ Å showing the diffuse scatter concentrated preferentially near the Bragg peaks.

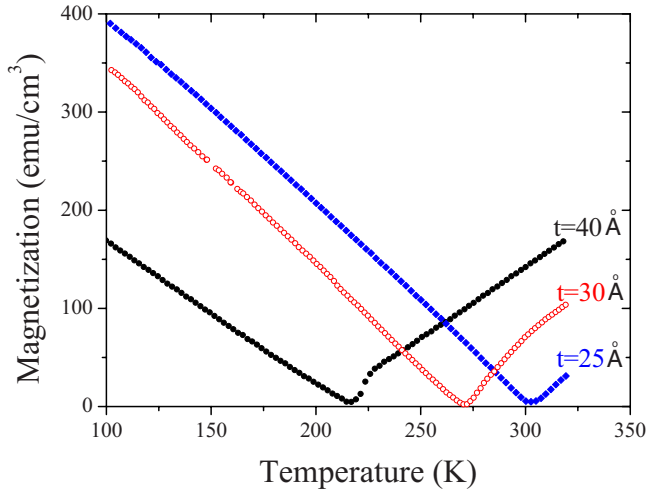


FIG. 4. (Color online) Magnetization as a function of temperature for three samples from the series $[\text{Co}_t/(\text{Gd}_{0.47}\text{Co}_{0.53})_{100 \text{ \AA}}]_{\times 20}/\text{Co}_t$ with $t=25 \text{ \AA}$ (\diamond), 30 \AA (\circ), and 40 \AA (\bullet) showing the tunability of the compensation temperature with thickness. Applied fields during the experiment were 50 Oe for $t=25 \text{ \AA}$ and $t=30 \text{ \AA}$ and 100 Oe for $t=40 \text{ \AA}$.

multilayer. The extension of the scattering to large in-plane q_x values shows that this conformality extends to short in-plane length scales resulting in a low correlation length typical of polycrystalline sputtered systems. The slight curvature of the diffuse Bragg sheets at high q_x results from refraction of the incident and/or scattered waves close to the critical angle.

B. Magnetic properties

One of the main features of ferrimagnetic Gd/Co alloys and multilayers is the existence of a temperature for which the total moment of each magnetic sublattice is equal, giving rise to a compensation of the total magnetization. This is due to the dramatic change that the magnetization of Gd layers suffers with temperature between 0 and 300 K, in contrast with the almost constant value for Co. $\text{Gd}_{0.47}\text{Co}_{0.53}$ alloy behavior is similar to a pure Gd as its Curie temperature is also close to 300K.² Figure 4 includes magnetization as a function of temperature for different samples of the series: $t=25, 30,$ and 40 \AA . The compensation temperature varies as a function of Co thickness. The layer moment for the thicker Co layers is larger requiring a larger moment in the alloy layer (i.e., lower temperature) for the moments to be the same and compensation to be reached. Therefore, T_{comp} decreases as t is increased.

In principle, the layer with the largest moment will align to the applied field direction. Due to the differing behavior of the moments as a function of T , one would expect the alloy $\text{Gd}_{0.47}\text{Co}_{0.53}$ sublattice to be aligned with the field below the compensation temperature with the Co sublattice aligned antiparallel to it. This situation is reversed at temperatures above T_{comp} , although we will show in this paper that thermal hysteresis exists in this process for fields below a certain value. The tunability of T_{comp} with t in the multilayered system is smoother than in the case of thin single layer films of

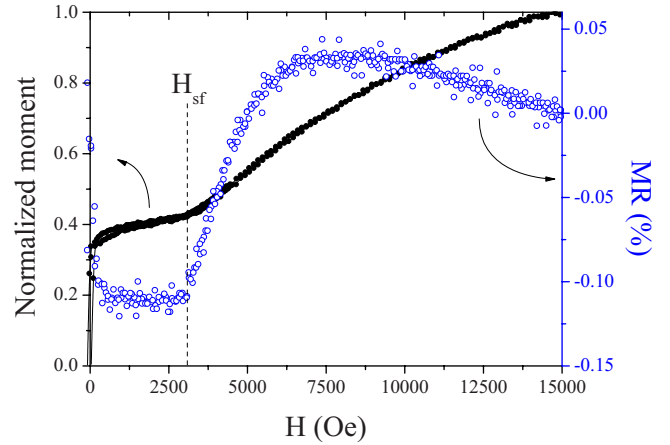


FIG. 5. (Color online) Normalized moment (left axis—full symbols) and magnetoresistance (MR) (right axis—open circles) measured at room temperature as a function of external field for sample with $t=35 \text{ \AA}$. Magnetization detects the appearance of the spin-flop transition as a change in the slope of the curve at the point marked. Although the overall change in MR is less than 0.15%, the transition is clearly seen by using this technique.

$\text{Gd}_{1-x}\text{Co}_x$ alloys, where compensation is only seen for x between 0.77 and 0.82.²

The system also presents other features usually associated with the Gd/Co or Gd/Fe systems such as the spin-flop transition, seen in Fig. 5 from both magnetoresistance (MR) and a magnetization loop (VSM). This transition arises from the competition in the system between the exchange energy, which tries to keep the layer moments antiparallel to the field, and the Zeeman term, which comes from the interaction with the external field and tries to align the layers parallel to it. The competition is especially apparent in systems with small anisotropy, where it causes the appearance in the system of a spin-flop transition that leads to a so-called twisted state.^{17–19} The moments of Gd and Co atoms rotate from their aligned direction to adopt a new configuration being almost $\pm 90^\circ$, but keeping the same total projected moment in the field direction. Further increasing the field allows the system to slowly rotate both moments toward it without increasing the exchange energy too much. The smaller the total moment of the sample M , the smaller the field required to enter this state, which is why it is easier to observe this transition near T_{comp} [Fig. 10 includes the temperature dependence of the field at which this transition occurs (H_{sf}) for the sample with $t=40 \text{ \AA}$]. The transition shown in both the M - H and MR loops in Fig. 5 marks the spin-flop transition in sample $t=35 \text{ \AA}$. The MR reflects mainly the changes in the resistance of the Co layers because the alloy layers are highly resistive due to their amorphous structure.⁸ The increase in spin disorder at H_{sf} induces an increase in resistivity. Above this transition, the magnetic field slowly rotates the moments of both sublattices toward its direction, reducing this disorder and therefore the resistivity of the sample.

Another feature typical of this kind of system, which has been studied very recently, is the thermal hysteresis effect. Although this is an old subject, its recent appearance in mul-

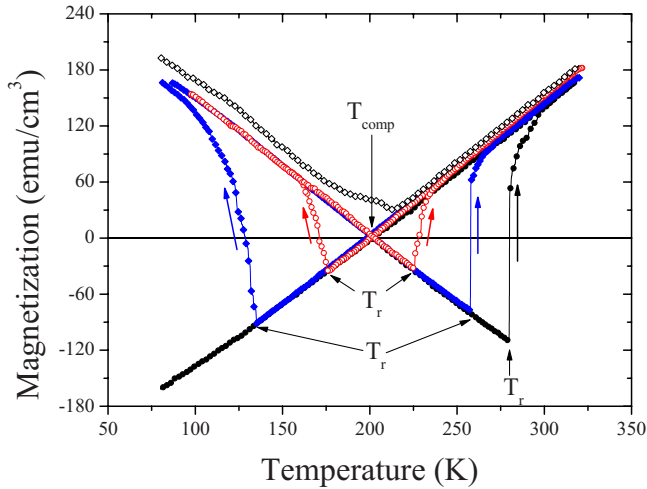


FIG. 6. (Color online) Magnetization as a function of temperature both heating and cooling the sample with $t=40$ Å under different magnetic fields: $H=10$ (●), 20 (◆), 40 (○), and 500 Oe (◇). The field was applied along the easy axis. The direction of each measurement is indicated by arrows, as well as the position of compensation (T_{comp}) and reversing (T_r) temperatures in each case. Thermal hysteresis is seen in all cases except $H=500$ Oe (see text).

tilayered systems^{11–13} has rekindled interest in recent years as it is easy to measure using conventional magnetometry as VSM, it may be very large (up to 150 K), and can be tuned or even eliminated as a function of the external field. The measurement of the magnetization as a function of temperature during both cooling and heating the sample in moderate fields gives rise to a characteristic bow-tie pattern. This effect has been seen on (Fe,Co,CoNi)/Gd (Refs. 13 and 20) and at higher fields on Co/Tb.²¹ Now, we show that it also appears very clearly in the Gd_{0.47}Co_{0.53}/Co system. Due to the improved artificial structure of this system arising from the negligible interdiffusion, all the features associated with this effect are more clearly identified and studied than in the more miscible Gd/Co and Gd/Fe systems.

Figure 6 shows the magnetization vs temperature at low fields for the sample with $t=40$ Å. During cooling, the exchange interaction allows the initial Co-aligned structure to remain stable through the compensation temperature, $T < T_{comp}$. Here, the moment of the Gd_{0.47}Co_{0.53} sublattice still points opposite to the external field even though it is actually larger than the Co sublattice which gives rise to a state with a net negative magnetization. The energy cost associated with reversing the direction of the two sublattices explains the reversal of magnetization occurring at a temperature less than T_{comp} (which we will refer to as the reversal temperature T_r). In a similar way, when heating the sample, the Gd_{0.47}Co_{0.53} aligned state is also stable up to a second T_r , which is above T_{comp} . Figure 6 exemplifies too how T_r are dependent on the field applied during the measurement, for example, $T_r=173$ and 228 K for $H=40$ Oe, but $T_r=135$ and 261 K for $H=20$ Oe. T_{comp} may be defined in these cases as the central crossing of the heating and cooling curves (marked in the graph), where the total sample moment is zero and the two sublattices have identical moments. Using this definition, T_{comp} is independent of the applied external

field as it should be (its value is $T_{comp}=200$ K for the sample in Fig. 6). Once T_{comp} is fixed by choosing the appropriate ratio of thicknesses, it is readily seen how the thermal hysteresis width (the difference in the two reversal temperatures) can be tuned easily by choosing the appropriate value for the applied field. As the amount of energy gained by the reversal of the magnetic structure is proportional to the external field (Zeeman term), the smaller the field, the further the T_r is from T_{comp} . Above a certain value for the external field, it is theoretically predicted that the thermal hysteresis should disappear and this is observed experimentally for $H=500$ Oe data in Fig. 6. On the other hand, the asymmetric shape of this curve near T_{comp} is due to the spin-flop transition. The value of H_{sf} reduces as the temperature approaches T_{comp} . If, during a M vs T ramp, H_{sf} reaches a value smaller than the one set for the external field during the measurement, the sample experiences such a transition, yielding an increase of magnetization that generates the mentioned asymmetry. It is very remarkable how abrupt the transitions are, especially the ones at higher temperature when compared with previously published experimental results.^{13,21} The experimental data shown in this paper are closer to the theoretical results where a perfect interface is assumed. Again, this is due to the improved interfacial properties of the Gd_{0.47}Co_{0.53}/Co multilayers studied here.

It is also worth noting the difference for a given field in the position of the two T_r from T_{comp} and the magnetization values for those temperatures. This is especially clear in the curve for $H=10$ Oe data: if the two values for T_r were symmetric about T_{comp} , the value of T_r for the cooling curve would be at 118 K, as it is $T_r=282$ K on the heating curve, but it has not been observed above 80 K. To understand this, it is useful to consider the schematic outline of the layer and total moment directions shown in Fig. 7. Here, the Gd_{0.47}Co_{0.53} moment is represented by a thick arrow and Co moment by a thin one. Below these two arrows, the total moment of the sample is also represented. The direction of the applied field (H_{ap}) is also shown. Let us assume that Co magnetization is approximately constant over the temperature range of measurement (it actually changes by less than a 0.7%) and consider two points either side of T_{comp} on the M vs T curve with the same M , say M_0 . This means that at the lower temperature, the alloy moment is greater than the Co one by M_0 , while at the higher T , it is smaller than Co by the same amount. Hence, even though the total moment is the same, the energy barrier required to reverse the magnetization is higher at the lower temperature as the moments to be rotated are larger. Therefore, both asymmetries (position and deepness of minima) are a consequence of the Gd_{0.47}Co_{0.53} sublattice magnetization being higher at lower T . This could also explain why the jump above T_{comp} is usually sharper than the one below compensation.

One of the reasons of studying Gd/Fe and Gd/Co multilayers is that Gd being an S ion presents a very small anisotropy. The Gd_{1-x}Co_x alloys share this property as they are amorphous for a very wide range of x . Furthermore, the coupling between Co and Gd is perfectly antiparallel, unlike the case for other rare earths as Tb or Dy.¹ This property simplifies the study of the interfacial interactions. As in previous studies, the thermal hysteresis effect is attributed to the

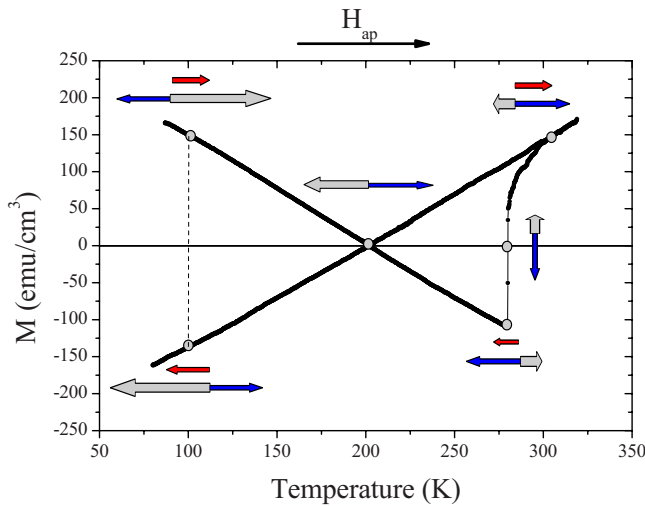


FIG. 7. (Color online) Schematic outline of the magnetic structure of each sublattice and total magnetization of the samples along a complete experimental M vs T loop. Thick arrow represents the total moment of the $\text{Gd}_{0.47}\text{Co}_{0.53}$ sublattice, the thin one corresponds to the Co sublattice, and the arrow below these two is associated with the total magnetization of the sample (note that it is zero at T_{comp}). The direction of the external field during the experiment is indicated on top of the figure. The dotted line compares two equivalent states (same T) before and after the magnetization reversal.

sample anisotropy, we have taken advantage of the natural uniaxial anisotropy that appears in the multilayers (mainly due to the Co polycrystalline layers) to study its effect on thermal hysteresis. A transversal MOKE magnetometer equipped with a rotary sample holder has allowed us to easily confirm the uniaxial anisotropy and to establish the easy and hard directions of anisotropy for each sample. The measurements corresponding to Fig. 6 were measured along the easy axis. The angle between easy and hard directions was always 90° . Once properly marked, VSM loops were also taken with the field applied along these two directions as a

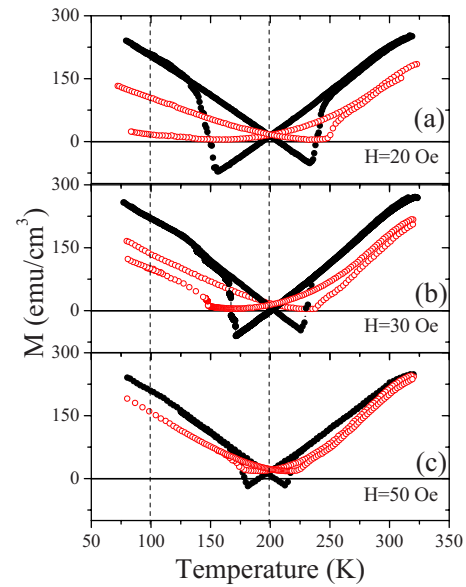


FIG. 9. (Color online) Thermal hysteresis loops taken in both easy (full circles) and hard (open circles) directions of the anisotropy on sample, with $t=40 \text{ \AA}$ at different fields: $H=20 \text{ Oe}$ [panel (a)], $H=30 \text{ Oe}$ [panel (b)], and $H=50 \text{ Oe}$ [panel (c)]. Note that the reversing temperature does not depend on anisotropy, but the shape of the minimum, corresponding to the reversing dynamics, is very different. Dotted line at 200 K marks the position of compensation temperature, independent of field and anisotropy.

function of temperature. Figure 8 shows some of these loops, including one near T_{comp} in panel (b). From the loop measured far from compensation [panel (a)], the coercive field (H_c) is well defined, and it is readily seen that although the magnetization process is very different for the easy and hard directions, the coercive field H_c is the same for both directions. In order to study the effect of this anisotropy on thermal hysteresis, Fig. 9 shows the M vs T recorded along the easy and hard directions at different fields ($H=20, 30,$ and 50 Oe) for the sample with $t=45 \text{ \AA}$. The shape of the curve is strongly dependent on the direction of measurement, al-

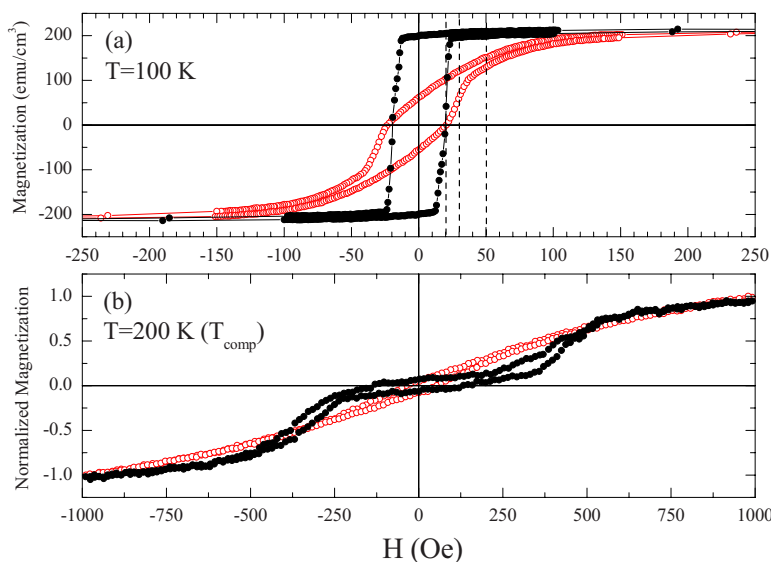


FIG. 8. (Color online) M - H loops taken with the sample aligned in the easy (full black circles) and hard (open red circles) directions for the sample with $t=40 \text{ \AA}$ recorded at different temperatures. Panel (a) shows the anisotropy well below compensation (100 K), while panel (b) presents the loops just at this temperature. The deformed shape caused by the spin-flop transition and the difficulty to extract the coercive field near this temperature are clear.

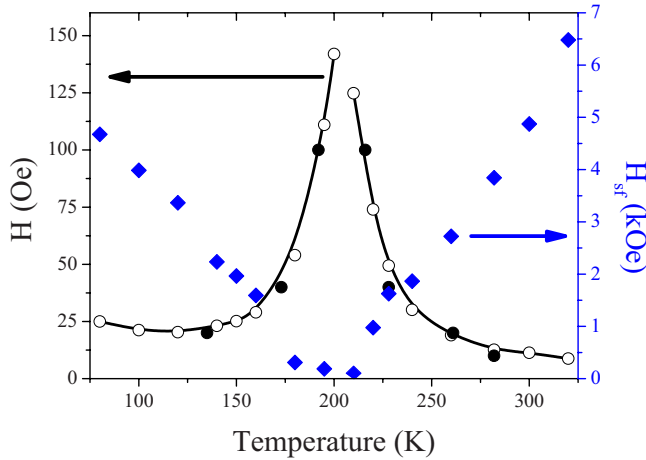


FIG. 10. (Color online) (Left axis) Coercive field of the sample with $t=40$ Å extracted from M - H loops along the range of temperatures available (open circles), and temperatures at which magnetization reversal takes place for the external fields employed (full circles). Spin-flop field (full diamonds—right axis) as a function of temperature presenting a minimum value at compensation

though we observe that the reversing temperature T_r , which in the hard direction may be associated with the point of minimum M , depends only on the applied field. To further clarify this point, we have measured the coercive field of the samples as a function of temperature. Figure 10 presents coercivity as a function of temperature and shows how its value increases as temperature approaches T_{comp} . In the same graph, the external magnetic field value set during the M vs T ramp for each pair of reversing temperatures (T_r) is included. It is clear how increasing the external field leads to reversing temperatures closer to T_{comp} . The two curves match quite well, which allows us to propose that it is the coercive field that is responsible for the spontaneous reversal at T_r . This point has not been previously reported as previous studies on thermal hysteresis in multilayers always refer to the anisotropy as the principal mechanism responsible for the effect.^{11,13} The spontaneous reversal from $-M_s$ to $+M_s$ with changing temperature observed in the M vs T curves (Figs. 5, 6, and 8) is somewhat equivalent to increasing the field from $-H$ to H during a M - H hysteresis loop. For this reason, the reversal in the hard direction is smoother than in the easy axis. Hysteresis loops shown in Fig. 8 reflect the same behavior. The shape of the magnetization loop in the hard axis [Fig. 8(a)] shows that the magnetization reversal is dominated by rotational processes rather than domain wall movement. The values of H employed during the M vs T curves (Fig. 9), recorded in the hard direction, are well below the saturation value resulting in the hard axis M vs T curves remaining below those recorded along the easy direction.

Also in Fig. 9, the heating and cooling curves corresponding to the field applied along the hard axis do not match at low temperatures, in contrast to those corresponding to the easy axis (see Fig. 6). This arises from the different types of hysteresis squareness observed in the M - H loops. The dashed lines in Fig. 8(a) mark the H values used for the measurement of the M vs T data plotted in Fig. 9; while they correspond to the saturated case for the easy axis direction, there are two possible states in the hard axis case due to the lower value of hysteresis squareness.

In general, reversing the magnetization reduces the total energy of the system due to the Zeeman interaction with the external field. As the total M of the system is reduced by approaching T_{comp} , this reduction of energy is smaller, so the field necessary for reversal is larger resulting in an increased H_c , which eventually diverges at T_{comp} (Fig. 10). Some difficulties arise when trying to measure coercivity at this temperature. First, as the moment tends to zero, the signal vanishes and the loop is lost preventing a reasonable value for H_c from being determined. Second, the presence of the spin-flop transition at lower fields near this temperature deforms the shape of the loop. Both features are clearly seen in the loop at T_{comp} in panel (b) of Fig. 8. Therefore, we do not give any experimental values of H_c for temperatures too close to T_{comp} in Fig. 10 as they may be misleading.

IV. CONCLUSIONS

We have shown that the $\text{Gd}_{0.47}\text{Co}_{0.53}/\text{Co}$ multilayered system is an excellent alternative to classical Gd/Fe or Gd/Co to study ferrimagnetic interactions in multilayers, due to its better defined interfaces. This system is shown to present all the characteristic features of Gd/Co or Gd/Fe multilayers, such as the existence of a compensation temperature, a spin-flop transition, and thermal hysteresis. We have measured the in-plane anisotropy of the samples and obtained thermal hysteresis loops as a function of field for easy and hard axes. We fully explain the reversal process and show that the temperatures at which the sample reverses its magnetization depend on the applied external field and coercivity, while anisotropy determines the smoothness of the reversal.

ACKNOWLEDGMENTS

The authors wish to acknowledge the support of P. Thompson and S. Brown at the XMAS beamline at ESRF and EPSRC for the provision of beamtime. J. A. González thanks the University of Castilla-La Mancha for funding through the “Ayudas de investigación para profesores a TC” programme.

- ¹P. Hansen, in *Handbook of Magnetic Materials*, edited by K. H. J. Buschow (North-Holland, Amsterdam, 1991), Vol. 6, p. 289.
- ²P. Hansen, C. Clausen, G. Much, M. Rosenkranz, and K. Witter, *J. Appl. Phys.* **66**, 756 (1989).
- ³A. H. Eschenfelder, in *Ferromagnetic Materials*, edited by E. P. Wohlfarth (North-Holland, Amsterdam, 1980), Vol. 2.
- ⁴S. Honda, M. Nawate, and I. Sakamoto, *J. Appl. Phys.* **79**, 365 (1996).
- ⁵J. B. Pelka, W. Paszkowicz, A. Wawro, L. T. Baczewski, and O. Seeck, *J. Alloys Compd.* **328**, 253 (2001).
- ⁶J. A. González, J. P. Andrés, M. A. López de la Torre, J. M. Riveiro, T. P. A. Hase, and B. K. Tanner, *J. Appl. Phys.* **93**, 7247 (2003).
- ⁷J. A. Gonzalez, J. Colino, J. P. Andres, M. A. L. de la Torre, and J. M. Riveiro, *Physica B* **345**, 181 (2004).
- ⁸J. A. González, J. P. Andrés, M. A. Arranz, M. A. López de la Torre, and J. M. Riveiro, *J. Appl. Phys.* **92**, 914 (2002).
- ⁹J. A. González, J. P. Andrés, M. A. Arranz, M. A. López de la Torre, and J. M. Riveiro, *J. Phys.: Condens. Matter* **14**, 5061 (2002).
- ¹⁰J. A. Alonso, R. Hojvat de Tendler, D. A. Barbiric, and J. M. Riveiro, *J. Phys.: Condens. Matter* **14**, 8913 (2002).
- ¹¹R. E. Camley, W. Lohstroh, G. P. Felcher, N. Hosoi, and H. Hashizume, *J. Magn. Magn. Mater.* **286**, 65 (2005).
- ¹²S. Demirtas, R. E. Camley, and A. R. Koymen, *Appl. Phys. Lett.* **87**, 202111 (2005).
- ¹³S. Demirtas, M. R. Hossu, R. E. Camley, H. C. Mireles, and A. R. Koymen, *Phys. Rev. B* **72**, 184433 (2005).
- ¹⁴M. Wormington, C. Panaccione, K. M. Matney, and D. K. Bowen, *Philos. Trans. R. Soc. London, Ser. A* **357**, 2827 (1999).
- ¹⁵J. P. Andres, L. Chico, J. Colino, and J. M. Riveiro, *Phys. Rev. B* **66**, 094424 (2002).
- ¹⁶D. E. Savage, J. Kleiner, N. Schimke, Y. H. Phang, T. Janowski, J. Jacobs, R. Kariotis, and M. G. Lagally, *J. Appl. Phys.* **69**, 1411 (1991).
- ¹⁷R. E. Camley, *Phys. Rev. B* **39**, 12316 (1989).
- ¹⁸C. Dufour, K. Cherifi, G. Marchal, P. Mangin, and M. Hennion, *Phys. Rev. B* **47**, 14572 (1993).
- ¹⁹W. Hahn, M. Loewenhaupt, Y. Y. Huang, G. P. Felcher, and S. S. P. Parkin, *Phys. Rev. B* **52**, 16041 (1995).
- ²⁰S. Demirtas and A. R. Koymen, *J. Appl. Phys.* **95**, 4949 (2004).
- ²¹M. R. Hossu and A. R. Koymen, *J. Appl. Phys.* **99**, 08C704 (2006).